

# Uncertainty in hydrologic impacts of climate change in the Sierra Nevada, California, under two emissions scenarios

Edwin P. Maurer

Received: 5 May 2005 / Accepted: 12 July 2006 / Published online: 28 February 2007  
© Springer Science + Business Media B.V. 2007

**Abstract** A hydrologic model was driven by the climate projected by 11 GCMs under two emissions scenarios (the higher emission SRES A2 and the lower emission SRES B1) to investigate whether the projected hydrologic changes by 2071–2100 have a high statistical confidence, and to determine the confidence level that the A2 and B1 emissions scenarios produce differing impacts. There are highly significant average temperature increases by 2071–2100 of 3.7°C under A2 and 2.4°C under B1; July increases are 5°C for A2 and 3°C for B1. Two high confidence hydrologic impacts are increasing winter streamflow and decreasing late spring and summer flow. Less snow at the end of winter is a confident projection, as is earlier arrival of the annual flow volume, which has important implications on California water management. The two emissions pathways show some differing impacts with high confidence: the degree of warming expected, the amount of decline in summer low flows, the shift to earlier streamflow timing, and the decline in end-of-winter snow pack, with more extreme impacts under higher emissions in all cases. This indicates that future emissions scenarios play a significant role in the degree of impacts to water resources in California.

## 1 Introduction

Climate change is affecting the water resources on which populations in the western US rely (e.g., Mote et al. 2005; Stewart et al. 2005; Trenberth et al. 2003), and continued anthropogenic emissions of greenhouse gases will exacerbate these effects for future decades and centuries (e.g., Dettinger et al. 2004; Hayhoe et al. 2004; Knowles and Cayan 2004; Stewart et al. 2004). Recognizing the crucial role management of water resources plays in sustaining California's economy (Draper et al. 2003), the high sensitivity of its ecosystems to climatic changes (Field et al. 1999), and the vulnerability of California's water supply to

---

E. P. Maurer (✉)  
Civil Engineering Department, Santa Clara University, Santa Clara, CA 95053-0563, USA  
e-mail: emaurer@enr.scu.edu

changes in precipitation or temperature, studies of the potential impact of climate change on California began nearly two decades ago. (Gleick 1987; Lettenmaier and Gan 1990).

The importance of this issue continues to generate considerable research using relatively coarse resolution Global Climate Models (GCMs) to drive land surface hydrology models (e.g., Brekke et al. 2004; Knowles and Cayan 2004; Maurer and Duffy 2005; Miller et al. 2003; Van Rheenen et al. 2004). Recent efforts using finer resolution regional climate models have attempted to define with more precision the spatial variability of anticipated changes in future hydroclimatology over California. (Kim et al. 2002; Kim 2005; Snyder et al. 2002). While there are many points of qualitative agreement between the wealth of studies on the topic, these studies tend to emphasize one or several selected potential outcomes, and the uncertainty in the projected impacts is not quantitatively addressed.

Quantifying the uncertainties in projections of climate change and its impacts is essential for assisting California policy-makers and water managers in adopting coherent and informed response strategies reflecting the state of scientific understanding of the likelihood of outcomes (Dettinger 2004; Kiparski and Gleick 2004). For assessing regional hydrologic impacts, one can consider four levels of uncertainty. The first three relate to the generation of regional climate information (Intergovernmental Panel on Climate Change, IPCC 2001) and consist of uncertainty in the future emissions of greenhouse gases, differing responses of GCMs to the resulting concentrations of these gases, and the uncertainty added by the downscaling technique used to translate the coarse scale GCM output to a regional spatial scale. Recent studies have also identified land use, implicit in the derived future emissions scenarios but not typically included in GCM simulations, as a potentially significant factor in regional climate (Feddema et al. 2005). This would add to the level of uncertainty of future regional climate effects represented by current GCM simulations included in this study. The fourth level of uncertainty relates to the selection and implementation of the land surface hydrology model. For regional hydrology impact studies, only recently have these differing sources of uncertainty been examined separately (e.g., Hayhoe et al. 2004; Wilby and Harris 2006; Zierl and Bugmann 2005).

Maurer and Duffy (2005) studied the projected regional impacts of rising CO<sub>2</sub> levels on California streamflow using GCM simulations performed between 1995 and 2002, archived as part of the Coupled Model Intercomparison Project (CMIP, Covey et al. 2003; Meehl et al. 2000). They examined only the second level of uncertainty outlined above, that is, the differing sensitivities of different GCMs under identically changing atmospheric conditions (a 1% per year CO<sub>2</sub> increase) to address the question of how variability in GCM responses affects the confidence with which we can expect different streamflow changes. In this study, more recent GCM simulations are used, reflecting the most recent improvements in model parameterizations and structures. In addition, the new GCM simulations are performed for many different SRES scenarios (rather than a fixed rate of increase in CO<sub>2</sub>), which allows comparison across different potential futures, addressing both the first and second levels of uncertainty discussed above.

Taking advantage of many new GCM simulations under different emissions scenarios, the following questions are posed: (1) What are the projected hydrologic impacts of climate change on Sierra Nevada mountain hydrology, and with what confidence, relative to the variability between GCMs, are these different from the base period of 1961–1990?; (2) With what confidence are the impacts under the two scenarios considered here different at the end of the century? These questions are addressed by forcing a land surface hydrology model with the future climate projected by different GCMs, and creating an ensemble of hydrologic responses under each emissions scenario.

## 2 Data and methods

### 2.1 Study region

The area of focus for this study is California, which is depicted in Fig. 1. In particular, the analyses that follow initially included four basins, the outlets of which are shown on Fig. 1. The basins drain western slopes of the Sierra Nevada mountain range, supplying fresh water to the extensive system of dams and reservoirs serving the water demands of much of the state. All four points are at inflows to large reservoirs. Characteristics of the four points identified in Fig. 1 are in Table 1, which shows the southern two basins (basins 3 and 4) contain more high elevation areas than the northern two (basins 1 and 2), and together a range of mean basin elevations is represented. Snow plays a crucial role in the management of seasonal water storage and delivery: On average the amount of water stored as snow in the Sierra Nevada (including only those areas that ultimately drain into the Sacramento–San Joaquin River system) on April 1, about  $12.4 \text{ km}^3$  (Hayhoe et al. 2004), is more than twice the total capacity of Lake Shasta, the largest manmade reservoir in California. Since one of the principal impacts of climate change on California water resources is on snowpack, and hydrologic changes exhibit a strong dependence on elevation (Knowles and Cayan 2004),

**Fig. 1** Location of the outlets to the four basins included in this study. Names indicate the river and the reservoir/dam into which the river discharges

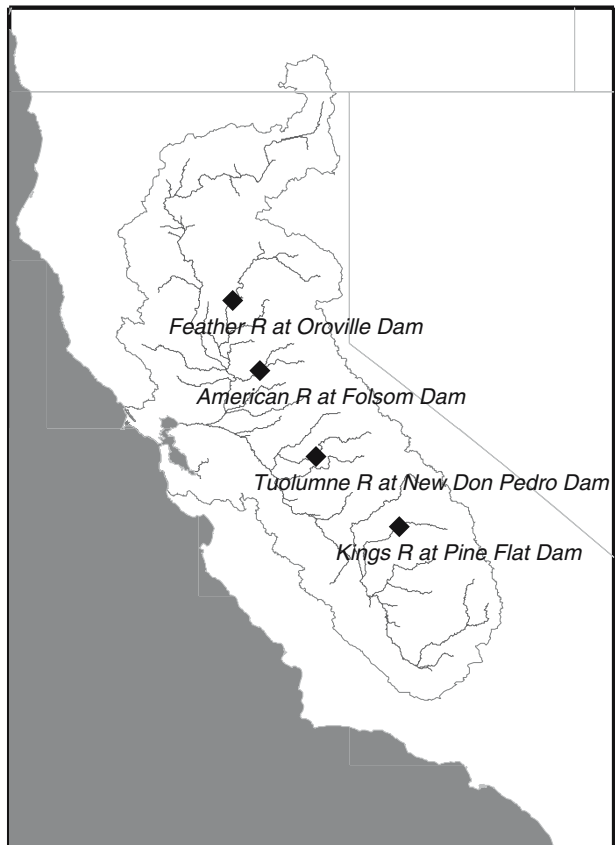


**Table 1** Locations and characteristics of the four basins in this study

Characteristic	Outlet point and basin characteristics			
	1. Feather R at Oroville	2. American R at Folsom Dam	3. Tuolumne at New Don Pedro Res	4. Kings R. at Pine Flat Dam
Latitude	39.522	38.683	37.666	36.831
Longitude	-121.547	-121.183	-120.441	-119.335
Drainage area (km <sup>2</sup> )	9,350	4,850	3,970	4,000
Mean basin elevation (m)	1,553	1,335	1,755	2,196
Max basin elevation (m)	2,655	3,009	3,802	4,086
Min basin elevation (m)	49	50	62	183

the selection of basins included in this study is designed to illuminate these differing responses.

## 2.2 Global climate models

Many international modeling groups have completed simulations of present climate and future climate under selected IPCC SRES scenarios in preparation for the IPCC 4th Assessment Report (AR4; Meehl et al. 2005). For this study, simulations are used from the 11 GCMs that by March 1, 2005 had completed and archived at least one simulation each of the twentieth century climate and future climate (through 2100) using emissions scenarios SRES A2 and B1. Updated output for those GCMs that revised their data was obtained in December 2005. These emissions scenarios are described in detail by Nakicenovic et al. (2000), where each scenario is built on a storyline that relates emissions to driving forces. A2, for example, is based on a world that is regionally organized economically, technological change is fragmented, and population growth is high. B1, by contrast, describes a world with low population growth and rapid changes in economies toward service and information, with relatively rapid introduction of clean and resource-efficient technologies. Each of these produces different atmospheric concentrations of greenhouse gases through the future centuries. While A2 does not represent the highest CO<sub>2</sub> emissions (at least through 2100) of the SRES scenarios (IPCC 2001), it is the highest emission scenario for which most modeling groups have completed simulations. As such, although it is by no means a “worst case,” A2 does represent the higher emission case in this study. B1 generally represents the best case of the SRES scenarios through the twenty-first century (IPCC 2001).

The GCMs included in this study are shown in Table 2. For each GCM, and each period (twentieth century, scenarios A2, B1) monthly precipitation (*P*) and temperature (*T*) data were obtained from the IPCC AR4 data archive hosted by the Program for Climate Model Diagnosis and Intercomparison. Where a GCM has archived more than one simulation under a particular scenario, only one simulation is used, so as not to bias the population of GCMs toward any specific model. All GCM results are interpolated onto a common 2°

**Table 2** GCMs included in this study

Modeling group, country	IPCC model ID	Abbreviation	Primary reference
Météo-France / Centre National de Recherches Météorologiques, France	CNRM-CM3	Cnrm	Salas-Mélia et al. 2005
CSIRO Atmospheric Research, Australia	CSIRO-Mk3.0	Csiro	Gordon et al. 2002
US Dept. of Commerce / NOAA / Geophysical Fluid Dynamics Laboratory, USA	GFDL-CM2.0	Gfdl	Delworth et al. 2005
NASA / Goddard Institute for Space Studies, USA	GISS-ER	Giss	Russell et al. 1995, 2000
Institute for Numerical Mathematics, Russia	INM-CM3.0	Inmcm	Diansky and Volodin 2002
Institut Pierre Simon Laplace, France	IPSL-CM4	Ipsl	IPSL 2005
Center for Climate System Research (The University of Tokyo), National Institute for Environmental Studies, and Frontier Research Center for Global Change (JAMSTEC), Japan	MIROC3.2 (medres)	Miroc	K-1 model developers 2004
Max Planck Institute for Meteorology, Germany	ECHAM5/ MPI-OM	Mpi	Junglaus et al. 2006
Meteorological Research Institute, Japan	MRI-CGCM2.3.2	Mri	Yukimoto et al. 2001
National Center for Atmospheric Research, USA	PCM	Pcm	Washington et al. 2000
Hadley Centre for Climate Prediction and Research / Met Office, UK	UKMO-HadCM3	hadcm3	Gordon et al. 2000

latitude–longitude grid, approximately equal to the spatial scale of the finest GCMs included in this study, to standardize the analysis that follows.

### 2.2.1 GCM bias correction and spatial downscaling

While large scale patterns of  $P$  and  $T$  simulated by state-of-the-art GCMs can be realistic, even the best models display biases on regional scales that are large enough to confound studies of the hydrologic impacts of climate change. To cope with this, many different techniques have been employed to process the raw GCM output to retain the large scale signal of the evolving climate simulated by the GCM while reproducing historical climate patterns on the landscape at local scales, an essential characteristic for meaningful hydrologic analysis (Wood et al. 2004). One method used in many studies is to use a shift or scaling factor derived by comparing a climate model's future  $P$  or  $T$  to its climatology, and to apply this shift to a historical record (e.g., Miller et al. 2003; Lettenmaier and Gan 1990). While that method effectively removes the bias of the mean GCM climatology from the future climate, it does not address the potential bias in the temporal variability of the climate model and constrains inter-annual variability to be constant.

For this study, we employ a bias correction technique originally developed by Wood et al. (2002) for using global model forecast output for long-range streamflow forecasting. This technique was later adapted for use in studies examining the hydrologic impacts of climate change (Hayhoe et al. 2004; Maurer and Duffy 2005; Payne et al. 2004; Van Rheeën et al. 2004). This is an empirical statistical technique that maps  $P$  and  $T$  during a historical period (1950–1999 for this study) from the GCM to the concurrent historical record. The historical data used in this study is gridded National Climatic Data Center Cooperative Observer

station data, developed as described in Maurer et al. (2002), and aggregated up to a 2° latitude–longitude spatial resolution. For  $P$  and  $T$ , empirical cumulative distribution functions (CDFs; Wilks 2006) are built for each of 12 months for each of the 2° grid cells for both the gridded observations and each GCM for the climatological period. For the entire simulation period the quantiles for GCM simulated  $P$  and  $T$  are then mapped to the same quantiles for the observationally based CDF. For example, if for one grid point the GCM  $P$  value in January of 2050 is equal to the median GCM value for January for 1950–1999, it is transformed to the median value for the gridded January observations for 1950–1999. For  $T$ , the linear trend is removed prior to this bias correction and replaced afterward, to avoid increasing sampling at the tails of the CDF as temperatures rise. Thus, the probability distribution of observations is reproduced by the bias corrected climate model data for the overlapping climatological period, while both the mean and variability of future climate can evolve according to GCM projections.

Climate model output, which at 200–500 km is at too large a scale for basin scale hydrologic analysis, requires spatial downscaling prior to its use in a hydrology model. This can be done with dynamical or statistical methods (see for example Benestad 2001; Mearns et al. 2001). The main disadvantage of dynamic downscaling is the computational effort involved, which renders its use impractical for extended transient simulations of multiple emissions scenarios and multiple GCMs, as used in this study. The method used in this study is that applied by Wood et al. (2002), which for each month interpolates the bias corrected GCM anomalies, expressed as a ratio (for  $P$ ) and shift (for  $T$ ) relative to the climatological period at each 2° GCM grid cell to the centers of 1/8° hydrologic model grid cells over California. These factors are then applied to the 1/8° gridded  $P$  and  $T$ .

As with any statistical downscaling method, some assumption of stationarity is needed. For the technique used in this study it is assumed that the processes shaping the climate at the fine grid scale during the 1950–1999 period will continue to govern local climate features in the future, which may not always be the case. Snyder et al. (2002) used a dynamic downscaling approach, employing a regional climate model to simulate a doubled CO<sub>2</sub> environment over California, and found temperature changes may be more extreme at higher elevations, for example. Kim (2005), also using a dynamical downscaling approach over California, projects increased occurrence of extreme precipitation events, which would not be captured by the approach as implemented in this study. However, for assessing hydrologic impacts, Wood et al. (2004) show that the statistical bias-correction/downscaling method as implemented here performs comparably to dynamical downscaling approaches, at least when assessing monthly and annual hydrologic statistics.

### 2.3 Hydrologic model simulations

The hydrologic model used in this study is the variable infiltration capacity (VIC) model (Liang et al. 1994; 1996). VIC is a macroscale, distributed, physically-based hydrologic model that balances both surface energy and water budgets over a grid mesh, typically at resolutions ranging from a fraction of a degree to several degrees latitude by longitude. One distinguishing characteristic of the VIC model is its use of a “mosaic” scheme, allowing a statistical representation of the sub-grid scale spatial variability in topography and vegetation/land cover, which is especially important when simulating the accumulation and ablation of snow in more complex terrain. To account for subgrid variability in infiltration, the VIC model uses a scheme based on the work by Zhao et al. (1980). The VIC model also features a nonlinear mechanism for simulating slow (baseflow) runoff

response, and explicit treatment of vegetation effects on the surface energy balance. The resulting runoff at each grid cell is routed through a defined river system using the algorithm developed by Lohmann et al. (1996).

The VIC model has been successfully applied in many settings, from global to river basin scale (e.g., Abdulla et al. 1996; Maurer et al. 2001, 2002; Nijssen et al. 1997, 2001), as well as in several studies of hydrologic impacts of climate change (Christensen et al. 2004; Hayhoe et al. 2004; Maurer and Duffy 2005; Payne et al. 2004; Wood et al. 2004). For this study, the model was run at a 1/8-degree resolution (measuring about 150 km<sup>2</sup> per grid cell) over the Sacramento–San Joaquin River system, using the identical parameterization as Van Rheeunen et al. (2004). As described by Maurer et al. (2002) the land use in the VIC hydrology model is static, being set at the level of the late twentieth century. While not included in this analysis, additional uncertainty would be introduced considering land conversion (such as agriculture to urban) as well as land cover changes induced by a warmer climate (Lenihan et al. 2003), since the projected hydrologic response changes with land cover assumptions. Since the focus of this study is on streams draining mountainous basins the prospect of dramatic land conversion would likely be small, though the hydrologic effects of other potential land cover changes remain to be established.

#### 2.4 Assessing uncertainty in hydrologic impact projections

Following the approach of Maurer and Duffy (2005), results for each impact, in this case streamflow and snowpack, for all GCMs are assembled for each emissions scenario. For each variable, the mean monthly value for each GCM for each of three defined periods is calculated, and these values for each GCM are combined by variable and period into ensembles. These ensembles of hydrologic variables are statistically analyzed using the non-parametric Mann–Whitney *U* test (Haan 2002) for equality of means to determine the confidence level for the change from the climatological period (1961–1990). In addition, the confidence with which it can be claimed that the two scenarios give different results is determined using the same test. Maurer and Duffy (2005) utilized a *t*-test for similar analyses, which assumes data follow a Gaussian distribution. While greater than 90% of the cases considered here can be considered Gaussian, applying a non-parametric test to all cases avoids the assumption of an underlying distribution for the data.

### 3 Results and discussion

For a domain including all four of the study basins the hydrologic model produced complete estimates of the water budget using each GCM. These were then summarized for four periods: the base period 1961–1990, 2011–2040, 2041–2070, and 2071–2100. To illustrate the scatter among the projections and impacts using the 11 GCMs for one basin under the A2 scenario, the results for the latter two periods are plotted in Fig. 2. This shows that there is a majority of GCMs showing increased winter *P*, but this is quite variable among the models, while the *T* increases appear more consistent. In general the impact on flow of these climatic changes is that winter flows increase and late spring and early summer flows decrease, with greater disagreement among models during the transition between the two. Declining snow water equivalent (SWE) is clear, and is more severe later in the century as temperatures continue to rise.

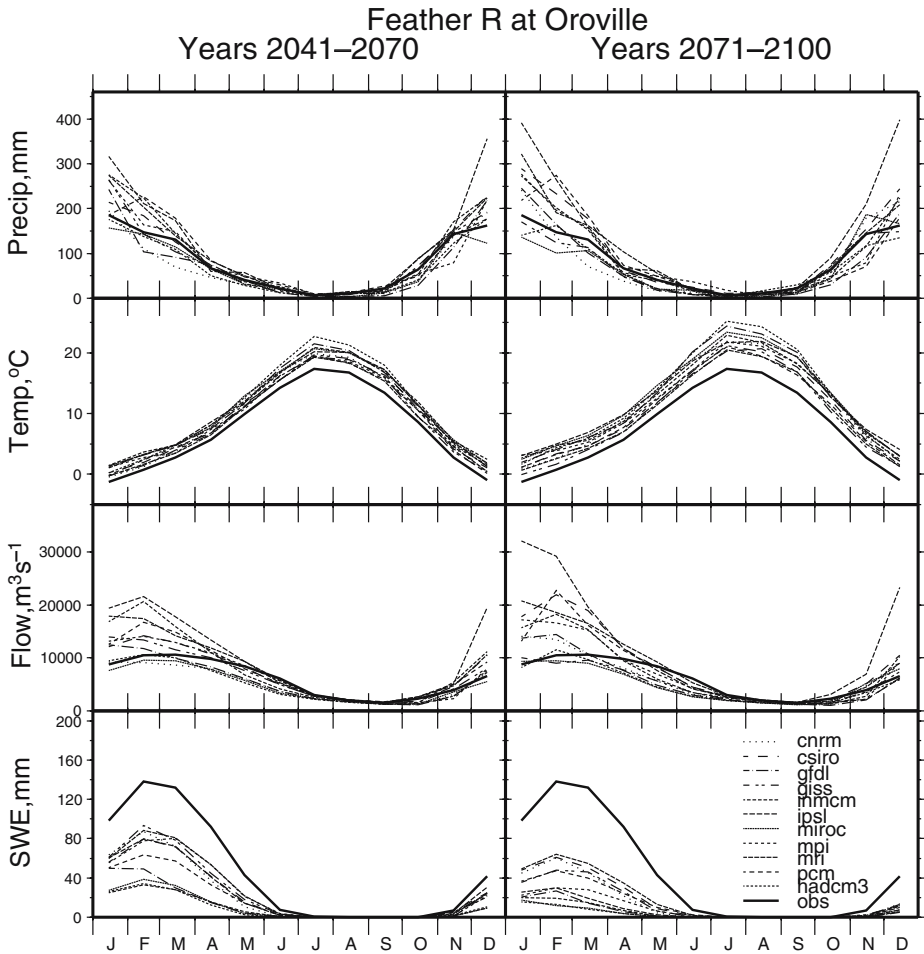


**Fig. 2** For one basin, for the SRESA2 scenario, the average precipitation and temperature, streamflow at the outlet point, and basin average snow water equivalent averaged over two 30-year periods. The *thicker line* labeled *obs* represents the baseline average for 1961–1990

### 3.1 Precipitation and temperature changes

To verify the observations above, and to use both emissions scenarios, Figs. 3 and 4 are shown. Note that the confidence thresholds highlighted in the Figures are comparable to the National Assessment Synthesis Team (2000) classification of “very likely or very probable” impacts as those with confidence >90%; the 67–90% category corresponds to “likely or probable” impacts. Since the changes in *P* were found to be remarkably consistent between basins, only the northern and southernmost basins are included in this section. Note that Fig. 3 shows the ensemble mean changes corresponding to the scatter of GCM traces in the top row of panels in Fig. 2.

The figures show for each month the mean *P* of the 1961–1990 base period and the change to each of the three future periods. Not shown in the figures is annual average *P*,

which exhibits small (about 5%) but significant (with 67–90% confidence) increases under the B1 emissions scenario in 2011–2040 and comparable decreases for 2041–2070. For all other cases, no statistically significant change in annual *P* is evident, though a pattern exists of slight increases in the north declining to slight decreases in the south. On a monthly level, Fig. 3 generally shows an increase in December–February *P*. A significant decline in April–June *P* is projected, and grows in magnitude later in the century, and the increase in winter *P* persists. Figure 4 shows a similar pattern toward the south, though with sharper declines in April–June *P* than in the north, and smaller increases in winter *P* especially later in the twenty-first century. Overall, the increase in winter *P* and decrease in spring *P* shifts the centroid of the annual precipitation volume 2–6 days earlier by 2071–2100.

While not shown, the *T* projections in the north and south are very close and are highly significant, even as early as 2011–2040. By the end of the twenty-first century, average annual *T* rises by 3.6–3.8°C for the A2 scenario, and 2.3–2.4°C for B1, with the greatest warming being in July with 3.0–3.1°C for the B1 scenario and 5.0–5.1°C for A2. While these changes are broad in scale, showing high consistency between the north and south, the differing characters of the basins produces different hydrologic responses.

To assess the separation of the future climate under the two SRES scenarios, the same statistical test for equality of means is performed between the A2 and B1 scenarios for 2071–2100. While both scenarios show highly significant changes in *T* by the end of the century, it is also found that the *T* rises are smaller for B1 as compared to A2 with statistical confidence exceeding 90% (with the exception of March for basins 2 and 4, where confidence is 87–88% that they differ). Differences in *P* projected under the two scenarios

**Fig. 3** Mean monthly precipitation and projected changes under the A2 and B1 emission scenarios for Basin 1 (see Table 1 for basin description). The upper panel is the base period (1961–1990) mean monthly precipitation. The lower two panels show three bars for each month, indicating mean changes relative to the base period for 2011–2040 (left bar), 2041–2070 (center bar), and 2071–2100 (right bar). Shading indicates the statistical confidence of the change using a Mann–Whitney U test

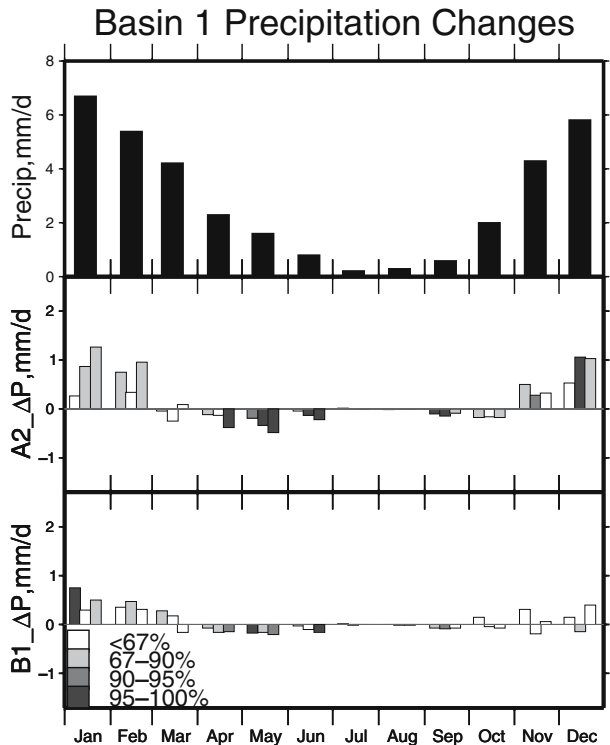
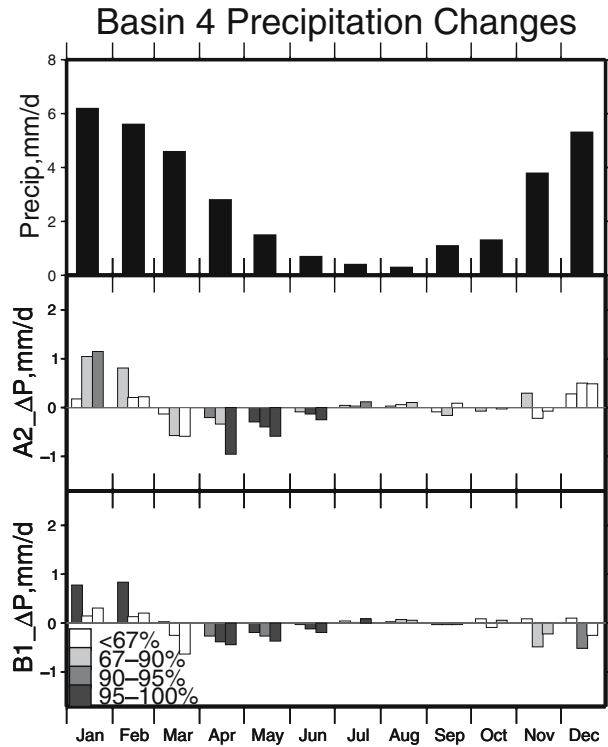


**Fig. 4** Same as Fig. 3, but showing the monthly precipitation and projected changes for Basin 4



are more complex. Table 3 shows the statistical confidence with which the 2071–2100 *P* differs for the two scenarios. For the annual average *P* the two scenarios produce statistically indistinguishable futures. Even at the monthly scale the differences in projected *P* for 2071–2100 under the two scenarios are not generally different with a high degree of confidence with the exception of April and May, where the decline in *P* projected under the A2 scenario is significantly greater than under B1.

**Table 3** Confidence that A2 and B1 mean *P* differs between 2071–2100 and the 1961–1990 base period

Month	Basin 1 (%)	Basin 2 (%)	Basin 3 (%)	Basin 4 (%)
Jan	51	60	60	67
Feb	44	42	35	15
Mar	48	20	23	23
Apr	96	98	99	99
May	84	78	76	76
Jun	75	68	63	66
Jul	38	0	3	31
Aug	0	49	49	31
Sep	16	13	3	8
Oct	42	49	45	45
Nov	25	20	15	40
Dec	39	39	52	35
Annual	18	10	3	0

Confidence is determined with the Mann–Whitney U test. Basin numbering is as in Table 1.

### 3.2 Streamflow and snow changes

The above changes in  $P$  and  $T$  produce changes in the hydrologic response of the landscape, which are reflected in the streamflow changes shown in Figs. 5 and 6. Note that Fig. 5 shows for basin 1 the ensemble mean flow changes corresponding to the GCM traces of flow in Fig. 2. For the lower elevation gauges, Fig. 5 shows high statistical confidence for the increases in December–February flows in all time periods, and the increases rise in magnitude through the century. This reflects the increasing  $P$  during these months under both scenarios as well as T-driven effects of increased proportions of  $P$  falling as rain instead of snow, and increased snow melt. The T-driven effects dominate, and more so as  $T$  increases continue, with changes in December–February  $P$  being 15–30% of the percent change in December–February flow, with the lower values toward the end of the twenty-first century. The increases in winter flows are markedly greater for the A2 scenario than B1, especially for 2071–2100. For A2, April–September flows decline, and the magnitude of this drop in flow increases through the twenty-first century. For B1 the same pattern is evident, but by 2071–2100 the declines in streamflow are less severe than under A2. Under the A2 scenario the increases in winter flow more than offset the declines in summer, producing a small (but low confidence) increase in annual flow for basins. The B1 scenario shows a similar effect for 2011–2040 with an increase in annual flow of 7–8% (with higher confidence of 67–90%); by 2071–2100 the B1 scenario shows a slight but low confidence decline in annual flow.

For the southern two basins at higher elevation, Fig. 6 illustrates the same pattern of changes for the southern basins. These show increased flows through April despite decreasing  $P$  in March and April. This is in contrast to the lower elevation northern basins,

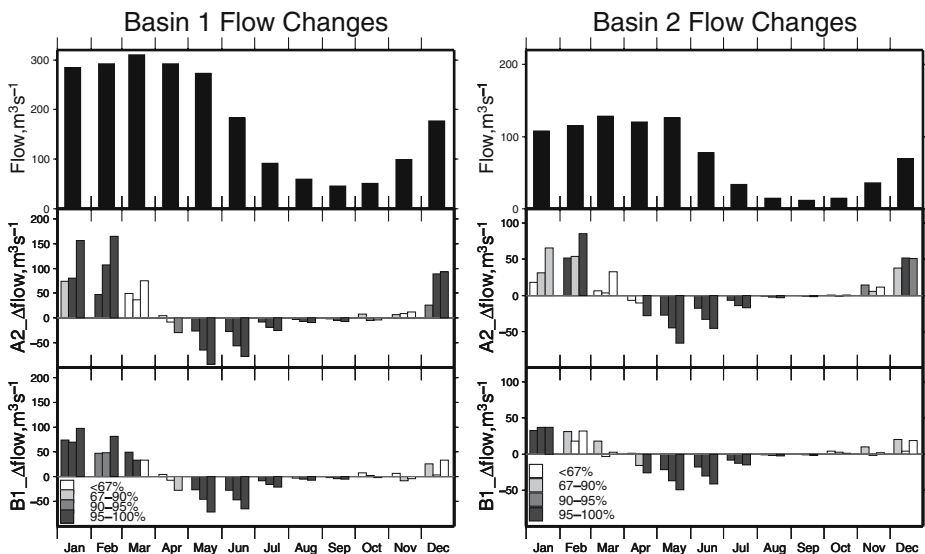


**Fig. 5** Similar to Fig. 3, this shows in the *top panel* the mean monthly flow for Basins 1 and 2, and the projected changes under the A2 (*center panels*) and B1 (*lower panels*) emission scenarios. *Shading* indicates statistical confidence. In the *lower two panels*, the three bars within each month indicate changes relative to the base period for early twenty-first century (2011–2040; *left bar*), mid-century (2041–2070; *center bar*) and end of century (2071–2100; *right bar*)

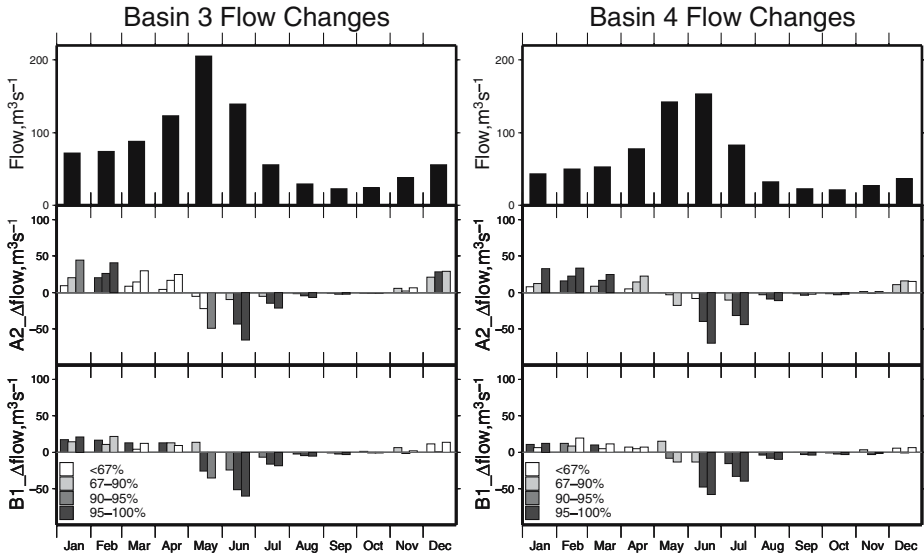


**Fig. 6** Same as Fig. 5 but for Basins 3 and 4

where flow increases continue only through March, with smaller declines and even some increasing *P*. This illustrates the interplay between *T* and *P* changes, where at higher elevation increases in December–February *P* can be stored as snow, later to augment flow. The statistically significant declines in late spring to early summer streamflow for 2071–2100 are limited to a shorter duration compared to the northern basins. Under the A2 scenario, the winter increase is offset by the late season decrease in flow, and the annual volume changes little. Under B1, the same pattern as in the north is seen, though by 2071–2100 the decreases in annual flow volume achieve higher confidence, especially basin 4.

The A2 and B1 emissions scenarios do not produce streamflows differing with a high degree of confidence, as shown in Table 4. The drops in May–August flow display the highest confidence that A2 and B1 result in different flow responses, with A2 showing sharper declines. The confidence in the difference between the scenarios is lower for the

**Table 4** Confidence that the mean flow for the A2 and B1 scenarios differ between 2071–2100 and the 1961–1990 base period

Month	Basin 1 (%)	Basin 2 (%)	Basin 3 (%)	Basin 4 (%)
Jan	60	30	56	63
Feb	48	52	48	48
Mar	56	60	44	49
Apr	44	<b>70</b>	48	56
May	<b>78</b>	<b>88</b>	35	25
Jun	<b>90</b>	<b>78</b>	63	<b>68</b>
Jul	<b>73</b>	<b>85</b>	60	<b>76</b>
Aug	<b>70</b>	<b>81</b>	57	<b>72</b>
Sep	63	55	28	44
Oct	25	18	0	30
Nov	44	62	60	47
Dec	44	52	20	10
Annual	15	30	10	0

Basin numbering is as in Table 1. Values larger than 67% are bold.

**Table 5** Mean April 1 SWE and percent change

April 1 SWE		SRESA2			SRESB1		
Basin	1961–1990 mean (mm)	2011–2040 $\Delta$ (%)	2041–2070 $\Delta$ (%)	2071–2100 $\Delta$ (%)	2011–2040 $\Delta$ (%)	2041–2070 $\Delta$ (%)	2071–2100 $\Delta$ (%)
1	114	<b>-38</b>	<b>-59</b>	<b>-80</b>	<b>-32</b>	<b>-46</b>	<b>-69</b>
2	121	<b>-29</b>	<b>-50</b>	<b>-71</b>	<b>-27</b>	<b>-38</b>	<b>-59</b>
3	305	-7	<b>-24</b>	<b>-39</b>	-7	<b>-22</b>	<b>-35</b>
4	360	-9	<b>-27</b>	<b>-43</b>	-8	<b>-24</b>	<b>-36</b>

Bold values indicate changes that exceed 95% confidence.

higher elevation southern basins showing declining sensitivity to the differences between A2 and B1 for the low flow period.

Table 5 summarizes the change in April 1 SWE for each basin for each time period. April 1 snowpack is a widely used indicator of the water available as summer supply in the western US (e.g., Hamlet and Lettenmaier 1999, Knowles and Cayan 2004); a decrease indicates either earlier melt and/or reduced winter snow accumulation. There is a clear pattern of lower snow loss for the southern, higher elevation basins, attributable to the fact that rising temperatures at higher elevations are less likely to bring temperatures above freezing and cause snow melt. Although there is significantly greater warming under A2, December–February  $P$  increases more dramatically for A2 than under B1 which results in small differences in April 1 SWE losses under the different emission scenarios through the early twenty-first century. By the mid–late twenty-first century, the  $T$  changes have become dominant, and B1 shows 11–13% less April 1 SWE loss compared to A2 at the lower elevation, northern basins. For the southern basins the difference in April 1 SWE loss is lower at 2–7%, showing that even with the projected  $T$  increases a substantial portion of the basins remain above the freezing level, thus  $T$  impacts on snow are lessened. All snow losses by mid-century are high confidence. The confidence level that the April 1 SWE loss projected under the two scenarios differs exceeds 80% for the lower elevation, northern basins, showing that while the impacts on April 1 SWE are high in all basins, the moderate elevation mountain basins will experience distinctly different snow impacts depending on future emissions pathways.

The earlier melt due to rising temperatures produces a shift in the date of the centroid of the annual flow volume, which is calculated using the center-of-mass approach of Stewart et al. (2004) and is shown in Table 6. Due to the compounding effects of increasing winter  $P$ , decreasing spring  $P$ , more winter  $P$  falling as rain instead of snow and earlier snow melt

**Table 6** Date of the centroid of the annual flow volume, and the shift in days

Flow centroid		SRESA2			SRESB1		
Basin	1961–1990 mean (days)	2011–2040 $\Delta$ (days)	2041–2070 $\Delta$ (days)	2071–2100 $\Delta$ (days)	2011–2040 $\Delta$ (days)	2041–2070 $\Delta$ (days)	2071–2100 $\Delta$ (days)
1	78	<b>-14</b>	<b>-18</b>	<b>-23</b>	<b>-10</b>	<b>-11</b>	<b>-17</b>
2	81	<b>-19</b>	<b>-23</b>	<b>-31</b>	<b>-17</b>	<b>-20</b>	<b>-26</b>
3	119	-9	<b>-20</b>	<b>-33</b>	<b>-10</b>	<b>-14</b>	<b>-23</b>
4	137	-9	<b>-21</b>	<b>-36</b>	<b>-8</b>	<b>-16</b>	<b>-24</b>

Mean is in day of year (January 1=1). Bold values indicate changes that exceed 95% confidence.

under higher  $T$ , there is a high degree of confidence that the shift is statistically significant for all basins and periods. Given the modest shift in the centroid of annual  $P$  (see Section 3.1), the shift in the centroid of the annual flow volume is predominantly due to  $T$  changes driving a greater proportion of rain and earlier snow melt. The continuing shift to earlier arrival of runoff later in the twenty-first century is robust for all basins, showing the effect of increasing  $T$  changes. Early in the twenty-first century the timing shift is highly significant but the differences between the A2 and B1 scenarios is less so, with confidence that the impacts under the A2 and B1 scenarios differ exceeding 75% only for the lower elevation basins. By 2041–2070, the shift for the B1 and A2 scenarios is different at the 90% confidence level for all but the highest elevation basin, basin 4. By 2071–2100 the confidence that the response differs under the two scenarios exceeds 90% for all basins, with the greatest difference in impacts seen at the higher elevation basins, showing that once the  $T$  change is great enough to affect the high elevation basins, impacts are more dramatic than for moderate elevation basins.

#### 4 Conclusions

For four basins in the Sierra Nevada in California, the simulated hydrologic impacts of future climate projected by 11 GCMs forced under two SRES emissions scenarios, a higher emission A2 and lower emission B1, were examined for statistical significance. While these scenarios do not represent worst and best case of possible emissions scenarios, of the selected SRES scenarios available for this study they do represent the generally bounding scenarios for twenty-first century CO<sub>2</sub> emissions. With this structure, this study addresses only uncertainty related to inter-GCM and inter-emissions scenario variability, not uncertainty due to the downscaling technique or the hydrology model transforming downscaled climate to streamflow. The two questions posed for this study are whether (and when) the projected hydrologic impacts have high statistical confidence (relative to the variability among GCMs), and whether the impacts under the two scenarios differs with high confidence.

Temperature ( $T$ ) shows highly significant increases over 1961–1990 levels, even early in the twenty-first century. By 2071–2100  $T$  rises by an average of 3.7°C under A2 and 2.4°C under B1, with July temperatures rising most dramatically by 5°C for A2 and 3°C for B1. The difference between the  $T$  increases, between 2071–2100 and 1961–1990, under A2 and B1 are highly significant. Thus it can be confidently stated that the emissions pathway we follow determines the future temperature experienced in the study region; alternatively, the choice of policies affecting future global emissions has a discernable impact in this region.

The same cannot be claimed so broadly for precipitation ( $P$ ). Increases in winter  $P$  and decreases in spring  $P$  are projected, both with generally higher magnitudes under A2 than B1, especially by 2071–2100. While annual  $P$  does not generally differ between the emissions scenarios, decreases in April–May  $P$  are significantly greater for A2 than B1.

For streamflow at the basin outlets, flow increases for December–March, and through April for higher elevation basins. Flows decline for April–September in the lower elevation basins, and May–October at higher elevations. Increases in winter and decreases in summer flow are both of greater magnitude under A2 than B1. The highest confidence in the differing response under A2 and B1 are for May–August declines in streamflow, where the decreases are sharper under A2 than B1.

By 2071–2100, the 36–80% losses in April 1 snow water equivalent (SWE) are highly significant for all basins, with greater losses at lower elevations. Greater losses under A2

than B1 are demonstrated with high confidence for lower elevation basins only, showing the changing sensitivity to emissions level with elevation.

The combined effects of changes in  $P$ ,  $T$  and SWE result in an earlier arrival of the annual flow volume by as much as 36 days by 2071–2100. For all basins, the difference in this shift for B1 emissions scenario is significantly less than for A2 by the end of the century.

In summary, as temperatures rise through the twenty-first century we can expect with high confidence an increase in winter streamflow from the Sierra Nevada, due primarily to temperature-driven effects of increasing proportion of rain versus snow and earlier snow melt, and secondarily to increasing winter  $P$ . We can also expect to experience a decrease in late spring and summer flow, which has important implications for California water management. We can confidently expect to have less water stored as snow at the end of winter, and we will expect an earlier arrival of the water, with implications on how reservoirs are managed. The emissions pathway, whether A2 or B1, shows some important differences in impacts, especially on the degree of warming expected, the decline in summer low flows, water stored as snow pack, and the shift to earlier streamflow timing, indicating that our emissions future determines to some extent the degree of impacts to water resources in California.

**Acknowledgements** The international modeling groups are acknowledged for providing their data for analysis, the Program for Climate Model Diagnosis and Intercomparison (PCMDI) for collecting and archiving the model data, the JSC/CLIVAR Working Group on Coupled Modelling (WGCM) and their Coupled Model Intercomparison Project (CMIP) and Climate Simulation Panel for organizing the model data analysis activity, and the IPCC WG1 TSU for technical support. The IPCC Data Archive at Lawrence Livermore National Laboratory is supported by the Office of Science, US Department of Energy.

## References

- Abdulla FA, Lettenmaier DP, Wood EF, Smith JA (1996) Application of a macroscale hydrologic model to estimate the water balance of the Arkansas-Red River basin. *J Geophys Res* 101(D3):7449–7459
- Benestad RE (2001) A comparison between two empirical downscaling strategies. *Intl J Climatol* 21: 1645–1668
- Brekke LD, Miller NL, Bashford KE, Quinn NWT, Dracup JA (2004) Climate change impacts uncertainty for water resources in the San Joaquin River basin, California. *J Am Water Resour Assoc* 40:149–164
- Christensen NS, Wood AW, Voisin N, Lettenmaier DP, Palmer RN (2004) The effects of climate change on the hydrology and water resources of the Colorado River basin. *Clim Change* 62:337–363
- Covey C, AchutaRao KM, Cubasch U, Jones P, Lambert SJ, Mann ME, Phillips TJ, Taylor KE (2003) An overview of results from the Coupled Model Intercomparison Project (CMIP). *Glob Planet Change* 37:103–133
- Delworth TL et al (2005) GFDL's CM2 global coupled climate models part 1: formulation and simulation characteristics. *J Climate* 19:643–674
- Dettinger M (2004) From climate-change spaghetti to climate-change distribution, Discussion Paper 500-04-028. California Energy Commission, Sacramento, California, p 20
- Dettinger MD, Cayan DR, Meyer MK, Jeton AE (2004) Simulated hydrologic responses to climate variations and change in the Merced, Carson, and American River basins, Sierra Nevada, California, 1900–2099. *Clim Change* 62:283–317
- Diansky NA, Volodin EM (2002) Simulation of present-day climate with a coupled atmosphere–ocean general circulation model. *Izv Atmos Ocean Phys (Engl Transl)* 38(6):732–747
- Draper AJ, Jenkins MW, Kirby KW, Lund JR, Howitt RE (2003) Economic-engineering optimization for California water management. *J Water Resour Plan Manage* 129(3):155–164
- Feddema JJ, Oleson KW, Bonan GB, Mearns LO, Buja LE, Meehl GA, Washington WM (2005) The importance of land-cover change in simulating future climates. *Science* 310(5754):1674–1678
- Field CB, Daily GC, Davis FW, Gaines S, Matson PA, Melack J, Miller NL (1999) Confronting climate change in California: ecological impacts on the golden state. Union of Concerned Scientists, Cambridge, Massachusetts, p 63

- Gleick PH (1987) The development and testing of a water balance model for climate impact assessment: modeling the Sacramento basin. *Water Resour Res* 23:1049–1061
- Gordon C, Cooper C, Senior CA, Banks HT, Gregory JM, Johns TC, Mitchell JFB, Wood RA (2000) The simulation of SST, sea ice extents and ocean heat transports in a version of the Hadley Centre coupled model without flux adjustments. *Clim Dyn* 16:147–168
- Gordon HB, Rotstayn LD, McGregor JL, Dix MR, Kowalczyk EA, O'Farrell SP, Waterman LJ, Hirst AC, Wilson SG, Collier MA, Watterson IG, Elliott TI (2002) The CSIRO Mk3 climate system model, CSIRO Atmospheric Research Technical Paper No.60, CSIRO. Division of Atmospheric Research, Victoria, Australia, p 130
- Haan CT (2002) *Statistical methods in hydrology*, 2nd edn. Iowa State Press, Ames, Iowa, USA, p 496
- Hamlet AF, Lettenmaier DP (1999) Effects of climate change on hydrology and water resources of the Columbia River basin. *J Am Water Resour Assoc* 35:1597–1624
- Hayhoe K, Cayan D, Field C, Frumhoff P, Maurer E, Miller N, Moser S, Schneider S, Cahill K, Cleland E, Dale L, Drapek R, Hanemann RM, Kalkstein L, Lenihan J, Lunch C, Neilson R, Sheridan S, Verville J (2004) Emissions pathways, climate change, and impacts on California. *Proc Natl Acad Sci USA* 101(34):12422–12427
- IPCC, 2001: *Climate Change 2001: the scientific basis. Contribution of Working Group I to the third assessment report of the Intergovernmental Panel on Climate Change*. In: Houghton JT, Ding Y, Griggs DJ, Noguer M, van der Linden PJ, Dai X, Maskell K, Johnson CA (eds) Cambridge University Press, p 881
- IPSL (2005) *The new IPSL climate system model: IPSL-CM4*. Institut Pierre Simon Laplace des Sciences de l'Environnement Global, Paris, France, p 73
- Jungclaus JH, Botzet M, Haak H, Keenlyside N, Luo J-J, Latif M, Marotzke J, Mikolajewicz U, Roeckner E (2006) Ocean circulation and tropical variability in the AOGCM ECHAM5/MPI-OM. *J Climate* 19:3952–3972
- K-1 model developers (2004) K-1 coupled model (MIROC) description, K-1 technical report, 1. In: Hasumi H, Emori S (eds) Center for Climate System Research, University of Tokyo, p 34
- Kim J (2005) A projection of the effects of the climate change induced by increased CO<sub>2</sub> on extreme hydrologic events in the western U.S. *Clim Change* 68:153–168
- Kim J, Kim TK, Arritt RW, Miller NL (2002) Impacts of increased CO<sub>2</sub> on the hydroclimate of the western United States. *J Climate* 15:1926–1943
- Kiparski M, Gleick PH (2004) Climate change and California water resources. In: Gleick PH (ed) *The World's Water 2004–2005*. Island Press, Washington, District of Columbia, pp 157–188
- Knowles N, Cayan DR (2004) Elevational dependence of projected hydrologic changes in the San Francisco estuary and watershed. *Clim Change* 62:319–336
- Lenihan JM, Drapek R, Bachelet D, Neilson RP (2003) Climate change effects on vegetation distribution, carbon, and fire in California. *Ecol Appl* 13(6):1167–1681
- Lettenmaier DP, Gan TY (1990) Hydrologic sensitivities of the Sacramento–San Joaquin River basin, California, to global warming. *Water Resour Res* 26:69–86
- Liang X, Lettenmaier DP, Wood E, Burges SJ (1994) A simple hydrologically based model of land surface water and energy fluxes for general circulation models. *J Geophys Res* 99(D7):14415–14428
- Liang X, Lettenmaier DP, Wood EF (1996) One-dimensional statistical dynamic representation of subgrid spatial variability of precipitation in the two-layer variable infiltration capacity model. *J Geophys Res* 101(D16):21403–21422
- Lohmann D, Nolte-Holube R, Raschke E (1996) A large-scale horizontal routing model to be coupled to land surface parameterization schemes. *Tellus* 48A:708–721
- Maurer EP, Duffy PB (2005) Uncertainty in projections of streamflow changes due to climate change in California. *Geophys Res Lett* 32:doi [10.1029/2004GL021462](https://doi.org/10.1029/2004GL021462)
- Maurer EP, O'Donnell GM, Lettenmaier DP, Roads JO (2001) Evaluation of the land surface water budget in NCEP/NCAR and NCEP/DOE reanalyses using an off-line hydrologic model. *J Geophys Res* 106(D16):17841–17862
- Maurer EP, Wood AW, Adam JC, Lettenmaier DP, Nijssen B (2002) A long-term hydrologically-based data set of land surface fluxes and states for the conterminous United States. *J Climate* 15(22):3237–3251
- Mearns LO, Hulme M, Carter TR, Leemans R, Lal M, Whetton P (2001) Climate scenario development. In: Houghton JT, et al (eds) *Climate Change 2001: the scientific basis. Contribution of working group I to the third assessment report of the intergovernmental panel on climate change*. Cambridge University Press, New York, pp 739–768
- Meehl GA, Boer GJ, Covey C, Latif M, Stouffer RJ (2000) The coupled model intercomparison project (CMIP). *Bull Am Meteorol Soc* 81(2):313–318
- Meehl GA, Covey C, McAvaney B, Latif M, Stouffer RJ (2005) Overview of the coupled model intercomparison project. *Bull Am Meteorol Soc* 86:89–93

- Miller NL, Bashford KE, Strem E (2003) Potential impacts of climate change on California hydrology. *J Am Water Resour Assoc* 39:771–784
- Mote PW, Hamlet AF, Clark MP, Lettenmaier DP (2005) Declining mountain snowpack in western North America. *Bull Am Meteorol Soc* 86:39–49
- Nakicenovic N, et al (2000) Special report on emissions scenarios. Cambridge University Press, Cambridge, UK
- Nijssen B, Lettenmaier DP, Liang X, Wetzel SW, Wood E (1997) Streamflow simulation for continental-scale basins. *Water Resour Res* 33(4):711–724
- Nijssen B, O'Donnell GM, Lettenmaier DP, Lohmann D, Wood EF (2001) Predicting the discharge of global rivers. *J Clim* 14:1790–1808
- Payne JT, Wood AW, Hamlet AF, Palmer RN, Lettenmaier DP (2004) Mitigating the effects of climate change on the water resources of the Columbia River basin. *Clim Change* 62:233–256
- Russell GL, Miller JR, Rind D (1995) A coupled atmosphere–ocean model for transient climate change studies. *Atmos–Ocean* 33:683–730
- Russell GL, Miller JR, Rind D, Ruedy RA, Schmidt GA, Sheth S (2000) Comparison of model and observed regional temperature changes during the past 40 years. *J Geophys Res* 105:14891–14898
- Salas-Méla D, Chauvin F, Déqué M, Douville H, Gueremy JF, Marquet P, Planton S, Royer JF, Tyteca S (2005) Description and validation of the CNRM-CM3 global coupled model. *Clim Dyn* (in review)
- Snyder MA, Bell JL, Sloan LC, Duffy PB, Govindasamy B (2002) Climate responses to a doubling of atmospheric carbon dioxide for a climatically vulnerable region. *Geophys Res Lett* 29(11), doi [10.1029/2001GL014431](https://doi.org/10.1029/2001GL014431)
- Stewart IT, Cayan DR, Dettinger MD (2004) Changes in snowmelt runoff timing in western North America under a 'business as usual' climate change scenario. *Clim Change* 62:217–232
- Stewart I, Cayan DR, Dettinger MD (2005) Changes toward earlier streamflow timing across western North America. *J Climate* 18:1136–1155
- Trenberth KE, Dai A, Rasmussen RM, Parsons DB (2003) The changing character of precipitation. *Bull Am Meteorol Soc* 84:1205–1217
- National Assessment Synthesis Team (2000) Climate change impacts on the United States: the potential consequences of climate variability and change on water resources of the United States. US Global Change Research Program, Washington, District of Columbia, p 151
- Van Rheeën NT, Wood AW, Palmer RN, Lettenmaier DP (2004) Potential implications of PCM climate change scenarios for California hydrology and water resources. *Clim Change* 62:257–281
- Washington WM, Weatherly JW, Meehl GA, Semtner AJ, Bettge TW, Craig AP, Strand WG, Arblaster J, Wayland VB, James R, Zhang Y (2000) Parallel climate model (PCM) control and transient simulations. *Clim Dyn* 16:755–774
- Wilby RL, Harris I (2006) A framework for assessing uncertainties in climate change impacts: low-flow scenarios for the River Thames, UK. *Water Resour Res* 42, W02419, doi [10.1029/2005WR004065](https://doi.org/10.1029/2005WR004065)
- Wilks DS (2006) Statistical methods in the atmospheric sciences, 2nd edn. Academic, San Diego, California, p 627
- Wood AW, Maurer EP, Kumar A, Lettenmaier DP (2002) Long range experimental hydrologic forecasting for the eastern U.S. *J Geophys Res* 107(D20):4429
- Wood AW, Leung LR, Sridhar V, Lettenmaier DP (2004) Hydrologic implications of dynamical and statistical approaches to downscaling climate model outputs. *Clim Change* 62:189–216
- Yukimoto S, Noda A, Kitoh A, Sugi M, Kitamura Y, Hosaka M, Shibata K, Maeda S, Uchiyama T (2001) The new Meteorological Research Institute coupled GCM (MRI-CGCM2) – model climate and variability. *Pap Meteorol Geophys* 51:47–88
- Zhao R-J, Fang L-R, Liu X-R, Zhang Q-S (1980) The Xin'anjiang model, in hydrological forecasting, proceedings, Oxford Symposium. *IAHS Publ* 129:351–356
- Zierl B, Bugmann H (2005) Global change impacts on hydrological processes in Alpine Catchments. *Water Resour Res* 41, doi [10.1029/2004WR003447](https://doi.org/10.1029/2004WR003447)